Available online at www.sciencedirect.com

SciVerse ScienceDirect

www.elsevier.com/locate/brainres

BRAIN RESEARCH

Research Report

Knockout of the γ-aminobutyric acid receptor subunit α4 reduces functional δ-containing extrasynaptic receptors in hippocampal pyramidal cells at the onset of puberty

Nicole Sabaliauskas[a], Hui Shen[b], Gregg E. Homanics[c], Sheryl S. Smith[b], Chiye Aoki[a,*]

[a]Center for Neural Science, New York University, New York NY 10003, USA
[b]Department of Physiology and Pharmacology, SUNY Downstate Medical Center, Brooklyn NY 11203, USA
[c]Deparments of Anesthesiology and Pharmacology and Chemical Biology, University of Pittsburgh, Pittsburgh PA 15261, USA

ARTICLE INFO

Article history:
Accepted 14 February 2012
Available online 22 February 2012

Keywords:
Puberty
GABA type A receptor
THP
Tonic inhibition
Alpha 4
Delta
Allopregnanolone

ABSTRACT

Increased plasmalemmal localization of α4βδ $GABA_A$ receptors (GABARs) occurs in the hippocampal pyramidal cells of female mice at pubertal onset (Shen et al., 2010). This increase occurs on both dendritic spines and shafts of CA1 pyramidal cells and is in response to hormone fluctuations that occur at pubertal onset. However, little is known about how the α4 and δ subunits individually mediate the formation of functional, plasmalemmal α4βδ GABARs. To determine whether expression of the α4 subunit is necessary for plasmalemmal δ subunit localization at pubertal onset, electron microscopic-immunocytochemistry (EM-ICC) was employed. CA1 pyramidal cells of female α4 knockout (KO) mice were tested for plasmalemmal levels of the δ subunit within dendritic spine and shaft profiles at the onset of puberty. EM-ICC revealed that the α4 and δ subunits localize on dendritic spines and shafts at sites extrasynaptic to GABAergic input at pubertal onset in tissue of wild-type (WT) mice. At pubertal onset, plasmalemmal localization of the δ subunit is reduced 45.9% on dendritic spines, and 56.7% on dendritic shafts with KO of the α4 subunit, as compared to WT tissue, yet levels of intracellular δ immunoreactivity remain unchanged. The decline in plasmalemmal localization is manifested as decreased responsiveness to the GABA agonist gaboxadol at concentrations that are selective for δ-containing GABARs. Additionally, α4 KO mice have larger dendritic spine and shaft profiles. Our findings demonstrate that α4 subunit expression strongly influences the pubertal increase of δ subunits at the plasma membrane, and that genetic deletion of α4 serves as a functional knock-down of δ-containing GABARs.

1. Introduction

γ-aminobutyric acid receptors (GABARs) are ubiquitously expressed throughout the CNS, and are responsible for mediating the majority of fast and tonic inhibition. The variety of unique GABAR subunit combinations results in receptors with diverse biophysical properties. The localization patterns of GABAR subunits reveal that α1β2γ2 GABARs are the most frequently-occurring in the CNS (Wisden et al., 1992). GABARs containing the δ subunit (in lieu of the γ2 subunit) localize

* *Corresponding author at:* 4 Washington Place, Room 1056, New York, NY 10003, USA. Fax: +1 212 995 4011.
E-mail address: chiye@cns.nyu.edu (C. Aoki).

0006-8993/$ – see front matter © 2012 Elsevier B.V. All rights reserved.
doi:10.1016/j.brainres.2012.02.035

extrasynaptically, due to the lack of interaction of the δ subunit with the GABAergic postsynaptic density protein gephyrin (Liang et al., 2004; Liang et al., 2006; Studler et al., 2002; Wei et al., 2003). As compared to other GABARs, α4βδ GABARs exhibit a distinct pattern of localization, with lower total surface expression throughout the CNS and with high concentrations observed in the dentate gyrus of the hippocampus and the thalamus (Pirker et al., 2000; Sperk et al., 1997; Sur et al., 1999; Wisden et al., 1992). In contrast to the brief, saturating levels of GABA that synaptically-localized receptors are exposed to, extrasynaptic α4βδ GABARs are localized to sites displaced from GABA release (Wei et al., 2003), which results in the exposure to low-level, ambient GABA concentrations. This and their relative lack of desensitization enables them to much more effectively maintain a constant inhibitory tone for the neuron (Bianchi and Macdonald, 2003; Glykys and Mody, 2006; Glykys et al., 2007; Stell and Mody, 2002).

Numerous reports have shown that the surface expression of α4βδ GABARs increases with fluctuations in female gonadal steroids, observed across the ovarian cycle, throughout pregnancy, at the onset of puberty, and when hormone fluctuations are mimicked through both exogenous administration and withdrawal (Griffiths and Lovick, 2005b; Gulinello et al., 2001; Hsu and Smith, 2003; Maguire et al., 2005, 2009; Shen et al., 2005, 2007, 2010; Smith et al., 1998a,b; Zhou and Smith, 2007). The importance of α4βδ GABARs was highlighted in recent studies of female brains at puberty (Shen et al., 2007, 2010). The pubertal increase in α4βδ GABARs reduced hippocampal excitability, NMDA-generated EPSCs, and synaptic plasticity, which is likely responsible for the decline in hippocampus-dependent spatial learning found at that time (Shen et al., 2010). These reports also showed a heightened level of restraint stress-induced or stress steroid-induced anxiety-like behaviors at the onset of puberty, and that this phenomenon can be ameliorated with knockout (KO) of the δ subunit (Shen et al., 2007), suggesting that increased plasmalemmal localization of α4βδ GABARs in the pyramidal cells of the CA1 hippocampus has a functional relevance for mood and learning at the onset of puberty.

One question that remains to be answered is whether plasmalemmal localization of the δ subunit at puberty requires α4 expression. In order to test this, we assessed δ subunit immunoreactivity within CA1 hippocampal pyramidal cells of α4 KO mice by analyzing tissue harvested from females at the onset of puberty, which is when α4βδ GABARs increase to peak levels within wild-type (WT) brains (Shen et al., 2007).

In the principal cells of the thalamus and cerebellum, the δ subunit forms functional pentamers predominantly with the α4 or the homologous α6 subunit, respectively (Jones et al 1997; Sur et al 1999). Since the α6 subunit expresses solely in the cerebellum, it is not a potential partner for δ in the hippocampus (Laurie et al., 1992; Nusser et al., 1996, 1998). However, the α1 subunit can co-localize with the δ subunit, as seen in dentate gyrus interneurons (Glykys et al., 2007). Previous reports show that both the α1 and δ subunits express in pyramidal cells of the CA1 hippocampus (Nusser et al., 1996; Wisden et al., 1992). Therefore, it is possible that, for CA1 hippocampal pyramidal cells, the absence of α4 subunit expression could still lead to pentamerization of the δ subunit with the α1 subunit, resulting in trafficking of δ-containing GABARs from intracellular stores to the plasma membrane at pubertal onset. Since the majority of surface-trafficked, stable GABARs capable of leaving the endoplasmic reticulum are complete pentamers, if the δ subunit cannot oligomerize with another α subunit, surface expression of the δ subunit would not be expected to increase at puberty (Bencsits et al., 1999; Green and Millar, 1995; Kittler et al., 2002).

One working model compatible with all of these observations is that the α4 and α1 subunits compete as binding partners for δ. The hormone fluctuations accompanying pubertal onset promote expression of α4, which in turn promotes the formation of α4βδ GABARs. Our current study addresses whether the absence of the α4 subunit will impact the surface expression of the δ subunit.

The current study differs in multiple significant ways from previous studies that have analyzed δ subunit expression within α4 KO brains. First, the previous studies that have examined surface expression of the δ subunit in α4 KO mice have done so in the thalamus and dentate gyrus (Chandra et al., 2006; Suryanarayanan et al., 2011). In WT tissue, levels of α4βδ GABARs remain elevated continuously in these brain regions (Wisden et al., 1992). In contrast, the CA1 hippocampus of females at puberty exhibits hormone fluctuation-dependent transient rises in these GABARs at pubertal onset (Shen et al., 2007, 2010). Secondly, in the dentate gyrus, GABAergic current is inward (Staley and Mody, 1992); this is not the case for the CA1 hippocampus, where GABAergic current is outward (Staley and Mody, 1992). Thus, the effect of this current reversal on δ subunit expression in α4 KO tissue is yet unknown. Finally, previous studies examined changes in δ expression after ethanol administration or epileptic seizure, which may depend on mechanisms different from those evoked by the endogenous changes accompanying pubertal onset (Brooks-Kayal et al., 1998; Goodkin et al., 2008; Liang et al., 2008; Sundstrom-Poromaa et al., 2002; Wei et al., 2004). While our previous light microscopic analysis was limited to showing the expression of α4 and δ GABAR subunits in individual cell types (Shen et al., 2007), electron microscopic-immunocytochemistry (EM-ICC) allows for localization to be distinguished as plasmalemmal or intracellular. This classification elucidates potential functionality of α4- and δ-containing GABARs. Our findings demonstrate that α4 KO mice show reduced plasmalemmal localization of the δ subunit at pubertal onset, and that α4 KO serves as a functional knock-down of δ-containing GABARs.

2. Results

2.1. *CA1 hippocampal α4 subunit immunoreactivity in α4 KO mice, as revealed by light microscopy*

Light microscopic (LM) observations showed that expression of the α4 subunit was apparent in the CA1 field of the hippocampus of female WT pubertal mice (Fig. 1 A). In contrast, qualitative observations revealed that the corresponding region of female α4 KO brains at puberty (Fig. 1 B) showed negligible α4 immunoreactivity. In WT pubertal sections, prominent labeling for the α4 subunit in the CA1 hippocampus allowed for identification of pyramidal cells from the otherwise non-

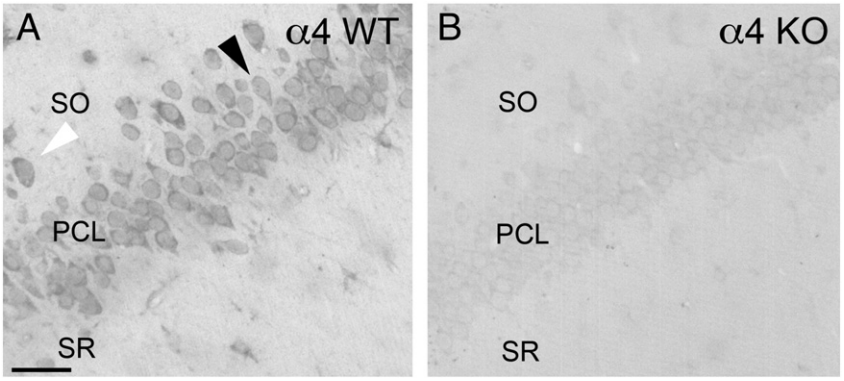

Fig. 1 – Light microscopic immunohistochemistry of α4 labeling in WT and α4 KO hippocampus. Light micrographs of hippocampal sections from WT and α4 KO pubertal female mice were captured following immunocytochemical labeling for the α4 subunit, using silver-intensified gold (SIG) as the label. Expression of the α4 subunit was apparent both in the pyramidal cell layer (PCL; black arrowhead) as well as in hippocampal interneurons (white arrowhead) of the stratum oriens (SO) and stratum radiatum (SR) of WT tissue (panel A). Qualitative analysis revealed marked reduction of the α4 subunit in α4 KO mice at puberty (panel B) when compared to the tissue of WT pubertal mice. Scale bar = 500 μm.

immunoreactive neuropil. Pyramidal cells were characterized as such by their triangular shape, small perikarya, and distinct apical dendrite descending into the stratum radiatum of the hippocampus. Interneurons in WT pubertal sections were also labeled for the α4 subunit, and were differentiated from pyramidal cells by their larger perikarya, rounded shape, and displacement from the pyramidal cell layer. Due to the dramatic reduction in α4 immunoreactivity in α4 KO brains, neither pyramidal cells nor interneurons were discernable from the surrounding neuropil. For quantitative analysis of subunit expression, we employed EM-ICC.

2.2. *α4 KO reduces immunoreactivity for the α4 subunit to levels comparable to primary antibody preadsorption controls*

To determine the specificity of the α4 antibody for the target protein, we performed a primary antibody preadsorption control. Upon incubation of the α4 primary antibody with the control peptide corresponding to the N-terminus region, we found a substantial reduction in plasmalemmal immunoreactivity in WT pubertal tissue by EM analysis. With α4 primary antibody preadsorption, plasmalemmal labeling was completely eliminated in WT pubertal dendritic spines ($p<0.00005$), and was reduced by 96.7% in WT pubertal dendritic shafts ($p<0.000001$). This finding indicates that the primary antibody we are utilizing is specific for the α4 subunit.

Previous studies indicate that the KO of the α4 subunit in this mouse strain was successful, citing a complete elimination of hippocampal α4 immunoreactivity by both western blot and light-microscopic immunohistochemistry (Chandra et al., 2006; Suryanarayanan et al., 2011). An EM-ICC characterization of this strain of α4 KO mice had not been performed until now. In our analysis of α4 KO tissue, we observed that the plasmalemmal α4 immunoreactivity on dendritic spines was reduced by 69.1% as compared to WT levels ($p<0.0001$; Figs. 2 A–C). Plasmalemmal immunoreactivity for the α4 subunit on dendritic shafts was reduced by 81.3% upon α4 KO ($p<0.000001$; Figs. 2 D–F). For both dendritic spines and dendritic shafts, the decrement of α4 immunoreactivity within the α4 KO was comparable to the low levels of labeling observed following omission of the primary antibody ($p>0.1$).

2.3. *Hippocampal pyramidal cells from WT and α4 KO mice exhibit normal neuronal phenotype*

We examined the phenotypes of CA1 hippocampal pyramidal cells from WT and α4 KO tissue by conducting LM analyses of two major neuronal phenotypes — immunoreactivity to α-amino-3-hydroxy-5-methyl-4-isoxazolepropionic acid (AMPA) receptor subunits GluR2/3, and to the microtubule-associated protein 2 (MAP2). CA1 pyramidal cells from pubertal WT and α4 KO mice exhibit equivalent levels of immunolabeling for both the GluR2/3 subunits and MAP2 (Figs. 3 A–D). Between the two genotypes, we also observed proper pyramidal cell morphology, and stratification of the CA1 hippocampus like that of WT tissue. Together, these data indicate that hippocampal neurons are likely to be developing normally and are capable of neurotransmission. As such, we concluded that any observed changes in localization of the δ subunit in the CA1 hippocampus at the onset of puberty in α4 KO mice are solely the result of the absence of α4 subunit expression.

2.4. *α4 KO hippocampus exhibits reduced δ subunit immunoreactivity at plasma membrane of dendritic spines and shafts at puberty*

EM-ICC data provide direct evidence for changes in plasmalemmal δ localization on CA1 pyramidal neurons upon KO of the α4 subunit. This technique also allows for distinguishing between localization at dendritic spines versus shafts and between synaptic versus extrasynaptic sites. On dendritic spine profiles, α4 KO resulted in a 45.9% reduction of plasmalemmal δ immunoreactivity as compared to spines of WT pubertal mice (Table 1; Figs. 4 A–C). EM analysis also revealed a significant reduction in plasmalemmal δ labeling on dendritic shafts of KO tissue, relative to the levels seen in WT mice. Labeling for the δ subunit at the dendritic shaft plasma membrane was reduced by 56.7% in tissue of α4 KO pubertal mice

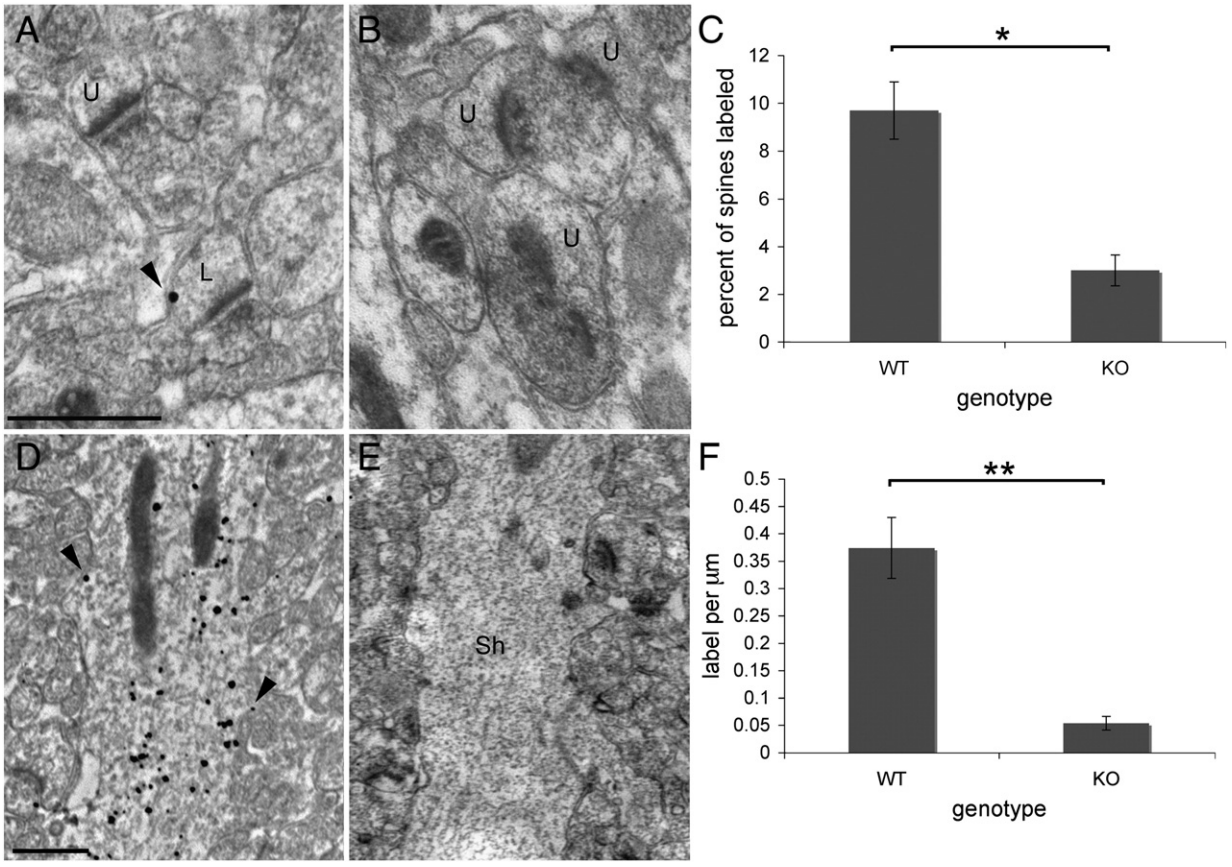

Fig. 2 – Plasmalemmal α4 immunoreactivity on pubertal CA1 hippocampal pyramidal cells' dendritic spines and shafts is reduced by α4 KO. Representative EM images of dendritic spine profiles from WT pubertal (panel A) and α4 KO pubertal (panel B) CA1 regions following SIG-immunocytochemistry to label α4 subunits. The black arrow denotes plasmalemmal SIG. 'U' denotes unlabeled dendritic spine profiles, while 'L' denotes a labeled dendritic spine profile. Scale bar for panels A and B = 500 nm. Mann–Whitney *U*-test of plasmalemmal α4 labeling revealed a significant effect of genotype, with significantly greater α4 immunoreactivity within WT pubertal tissue, compared to α4 KO pubertal tissue (panel C; *p < 0.0001). n = 1400 spines, sampled equally from 5 WT pubertal and 5 KO pubertal mice. Representative EM images of dendritic shafts from WT pubertal (panel D) and α4 KO pubertal (panel E) mice. The black arrow denotes plasmalemmal SIG. 'Sh' denotes dendritic shafts. Scale bar for panels C and D = 500 nm. Mann–Whitney *U*-test plasmalemmal α4 labeling revealed a significant effect of genotype, with significantly greater α4 immunoreactivity within WT pubertal tissue, compared to α4 KO pubertal tissue (panel F; **p < 0.000001). n = 200 dendrites sampled equally from 5 WT pubertal and 5 KO pubertal mice. Values indicate means ± SEM.

as compared to tissue of WT pubertal mice (Table 1; Figs. 4 D–F). These EM-ICC data demonstrate that α4 KO mice have reduced plasmalemmal localization of δ-containing GABARs on dendritic spines and shafts at pubertal onset as compared to WT mice.

In addition to allowing for differentiation between immunoreactivity on dendritic spines and shafts, EM-ICC also allows for the differentiation of synaptic versus extrasynaptic localization along the plasma membrane. In WT pubertal tissue, of the 93 SIG puncta found localized to the plasma membrane from 100 individual dendritic shaft profiles, only one puncta was localized synaptically, while three puncta were localized perisynaptically (within one axon terminal-width of the site of input). The remaining 90 puncta were outside of this boundary, and were classified as extrasynaptic. In α4 KO pubertal tissue, of the 46 plasmalemmal SIG puncta found on 100 dendrites, there were no synaptic puncta, and only one that was perisynaptic, with the remaining 45 localized extrasynaptically. These findings demonstrate that the localization of the δ-containing GABARs is predominantly extrasynaptic, regardless of expression of the α4 subunit.

2.5. *Levels of intracellular δ immunoreactivity are equivalent in α4 KO and WT hippocampal dendritic spines and shafts at puberty*

After establishing that α4 KO has an effect upon plasmalemmal localization of the δ subunit, we next sought to determine if α4 KO has an effect upon overall δ expression. We did so by comparing the amount of surface immunolabeling relative to the total labeling (surface + intracellular) between WT and α4 KO pubertal tissue. For both dendritic spines and dendritic shafts, we found a significantly higher ratio of surface-to-surface + intracellular immunolabeling in WT pubertal tissue than seen in α4 KO pubertal tissue (Table 1). This difference in ratio is likely due to the observed decrease in plasmalemmal δ localization upon α4 KO, but could be due to alterations

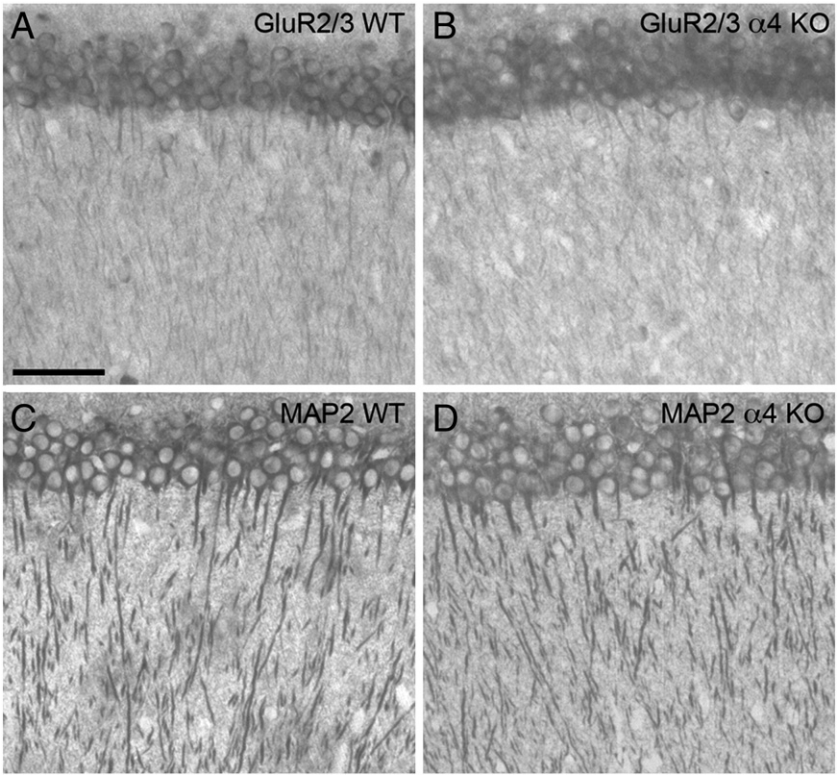

Fig. 3 – CA1 pyramidal cells exhibit a normal neuronal phenotype: A comparison of WT and α4 KO pubertal mice. Light microscopy reveals normal expression levels of two neuronal markers. Expression levels of the AMPA receptor subunit GluR2/3 are indistinguishable between WT pubertal (panel A) and α4 KO pubertal (panel B) tissue. Pubertal tissue of WT (panel C) and α4 KO (panel D) mice also showed similar immunoreactivity to the neuronal marker MAP2. The CA1 hippocampus from both genotypes also exhibits proper pyramidal cell morphology and stratification. Scale bar for panels A–D = 500 μm.

in intracellular immunoreactivity. To test this possibility, we measured levels of intracellular δ immunoreactivity in dendritic spines and shafts of α4 KO tissue and compared these levels to those found in WT pubertal tissue. In dendritic spine profiles, α4 KO pubertal mice showed equivalent levels of intracellular δ immunoreactivity as compared to WT pubertal mice (Table 1). We also found no difference in intracellular δ labeling in dendritic shafts between WT and KO pubertal tissue (Table 1). With the equivalent levels of intracellular immunoreactivity between the two genotypes, these EM-ICC data demonstrate that while plasmalemmal localization of the δ subunit on dendritic spines and shafts is compromised in α4 KO, levels of δ-containing GABARs within dendritic spines and shafts at pubertal onset are equivalent in α4 KO and WT pubertal mice.

2.6. *α4 KO hippocampus exhibits larger dendritic spine and shaft profiles*

Bigger spines would be expected to have more labeling, simply because they occupy more area and membrane within which to potentially express the δ subunit. Was the observed genotype difference in δ immunoreactivity of spines simply due to differences in the size of spines? In order to answer this, we first measured the area and membrane lengths of dendritic spine profiles, as captured in single (not 3D reconstructed)

Table 1 – δ subunit immunoreactivity in CA1 hippocampal pyramidal cell dendritic spines and shafts at puberty.

	δ immunoreactivity	WT Mean ± SEM (n)	KO Mean ± SEM (n)	p-value * (Z)
Spines	Surface (percent labeled)	5.16 ± 0.83 (700)	2.79 ± 0.70 (700)	**0.00008 (3.955)**
	Intracellular (percent labeled)	4.92 ± 0.86 (700)	4.22 ± 0.91 (700)	0.5 (−0.629)
	Surface proportion of total labeling (percent)	59.9 ± 6.5 (54)	36.3 ± 7.0 (45)	**0.03 (2.091)**
Shafts	Surface (label per μm)	0.097 ± 0.011 (100)	0.042 ± 0.009 (100)	**0.00006 (−4.402)**
	Intracellular (label per μm^2)	1.151 ± 0.085 (100)	1.021 ± 0.070 (100)	0.5 (−0.715)
	Surface proportion of total labeling (percent)	0.147 ± 0.016 (100)	0.047 ± 0.011 (100)	**0.00001 (−4.921)**

* Bold numbers indicate significant p-values.

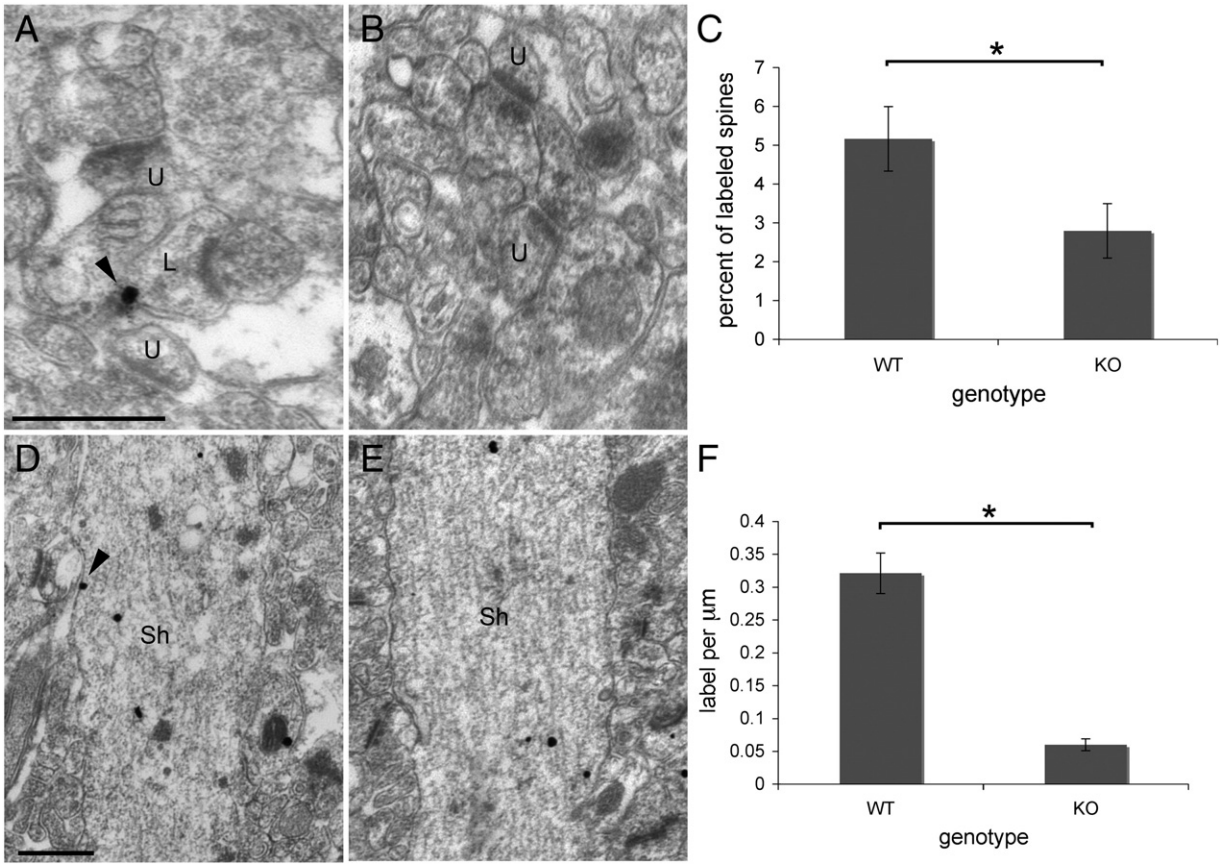

Fig. 4 – Plasmalemmal δ immunoreactivity on pubertal CA1 hippocampal pyramidal cells' dendritic spines and shafts is reduced by α4 KO. Representative EM images of dendritic spine profiles from WT pubertal (panel A) and α4 KO pubertal (panel B) CA1 regions following SIG-immunocytochemistry to label δ subunits. The black arrow denotes plasmalemmal SIG. 'U' denotes unlabeled dendritic spine profiles, while 'L' denotes a labeled dendritic spine profile. Scale bar for panels A and B = 500 nm. Mann–Whitney *U*-test of plasmalemmal δ labeling revealed a significant effect of genotype, with significantly greater δ immunoreactivity within WT pubertal tissue, compared to α4 KO pubertal tissue (panel C; *p < 0.0001). n = 1400 spines, sampled equally from 5 WT pubertal and 5 KO pubertal mice. Representative EM images of dendritic shafts from WT pubertal (panel D) and α4 KO pubertal (panel E) mice. The black arrow denotes plasmalemmal SIG. 'Sh' denotes dendritic shafts. Scale bar for panels C and D = 500 nm. Mann–Whitney *U*-test of plasmalemmal δ labeling revealed a significant effect of genotype, with significantly greater δ immunoreactivity within WT pubertal tissue, compared to α4 KO pubertal tissue (panel F; *p < 0.0001). n = 200 dendrites sampled equally from 5 WT pubertal and 5 KO pubertal mice. Values indicate means ± SEM.

digitized images from pubertal WT and α4 KO tissue. Between the genotypes, we found that larger spines occurred in α4 KO mice, as indicated by increases in both spine head area and membrane length (Table 2). Therefore, the fact that α4 KO mice have less surface labeling despite having more membrane length strengthens the argument that plasmalemmal localization of the δ subunit is dependent upon α4 subunit expression. As intracellular labeling between WT and α4 KO spines is unchanged, despite the larger spine area in α4 KO tissue, it is likely that the δ subunits that cannot localize to the plasma membrane contribute to the intracellular pool in α4 KO tissue.

As the dendritic shaft area and membrane length vary depending upon the plane of the dendrite within the ultrathin section, we measured the minimal diameter of the dendritic shaft profiles from single digitized images to estimate the

Table 2 – Morphological parameters for dendritic spines and shafts of CA1 pyramidal cells.

Pyramidal cell parameters		WT Mean ± SEM (n)	KO Mean ± SEM (n)	p-value * (Z)
Spines	Spine area (nm^2)	64319 ± 1743 (500)	72308 ± 1796 (500)	**0.00005 (4.080)**
	Spine membrane (nm)	1012 ± 15 (500)	1070 ± 15 (500)	**0.001 (3.287)**
Shafts	Diameter (nm)	1504 ± 35 (100)	1609 ± 42 (100)	**0.05 (−1.985)**

* Bold numbers indicate significant p-values.

relative size of shafts. We found that α4 KO mice also have larger apical dendritic shafts as compared to WT mice (Table 2). This increase in diameter would result in a modest increase in the membrane length and membrane area of each dendrite. However, since our measurements for immunoreactivity in and on dendritic shafts are calculated as densities (SIG per μm for surface, and SIG per μm^2 for intracellular), the difference in size between WT and α4 KO tissue is not a factor for our calculations.

2.7. *Hippocampal pyramidal cells of pubertal α4 KO mice show a reduced response to the GABAR agonist, gaboxadol at a concentration specific for the δ-containing GABAR*

Our EM-ICC data demonstrate that plasmalemmal localization of the δ GABAR subunit is compromised at the onset of puberty upon elimination of α4 subunit expression. As such, the functionality of δ-containing GABARs would be expected to decrease. In order to test this prediction, hippocampal slices from WT and α4 KO pubertal mice were analyzed for functional δ-containing GABAR expression electrophysiologically. Tonic currents were recorded from pyramidal cells in hippocampal slices using whole cell patch clamp procedures. Administration of 100 nM of the GABAR agonist gaboxadol (GBX), which targets only δ-containing GABARs (Brown et al., 2002; Meera et al., 2011), revealed a robust increase in inhibitory current in slices from WT pubertal mice, but only a minimal response in slices from α4 KO pubertal mice (Figs. 5 A and B). Subsequent application of the GABAR antagonist gabazine (GBZ), which blocks all GABARs at a concentration of 120 μM, resulted in a restoration of holding current to pre-GBX levels in both WT and α4 KO pubertal slices, indicating that GBX is targeting only GABARs. Our data are in agreement with previously reported findings, which demonstrated decreased GBX sensitivity in ventrobasal thalamic neurons of α4 KO animals (Chandra et al., 2006). These findings indicate that high expression levels of extrasynaptic α4βδ GABARs contribute to the tonic current in WT pubertal hippocampus, and are in agreement with EM-ICC data, demonstrating that there still are δ-containing GABARs expressing in α4 KO mice at puberty, but their levels are reduced from those seen in WT mice at puberty.

3. Discussion

By comparing δ immunoreactivity in WT and α4 KO pubertal mice, we found that elimination of α4 subunit expression reduced plasmalemmal localization of δ-containing GABARs in the CA1 hippocampus dendritic shaft and spine profiles at the onset of puberty.

3.1. *α4 KO reduces α4 immunoreactivity in the CA1 hippocampus*

Previous reports indicate that KO of the α4 subunit resulted in elimination of α4 expression in the dentate gyrus of the hippocampus (Chandra et al., 2006; Suryanarayanan et al., 2011). Our data also reveal that α4 immunoreactivity is extremely low in both α4 KO tissue and upon primary antibody preadsorption of WT tissue. The residual immunoreactivity in α4 KO tissue was not further reduced with primary antibody preadsorption. Therefore, the trace amount of α4 labeling seen in α4 KO tissue is most likely due to non-specific antibody binding, and that α4 protein expression is indeed absent in α4 KO mice.

3.2. *α4 knockout impairs plasmalemmal δ localization in the CA1 hippocampus at the onset of puberty*

The discovery that α4 KO mice show reduced plasmalemmal localization of δ subunits on dendritic spine and shaft profiles compared to WT mice has two possible interpretations: First, it is possible that in the absence of α4 expression, the δ subunit can co-localize with the α1 subunit, forming α1βδ GABARs. This is supported by data from other labs, which show expression of α1βδ GABARs occurring on interneurons of the dentate gyrus (Glykys et al., 2007). Second, it is possible δ subunits localize to the plasma membrane in the absence of other

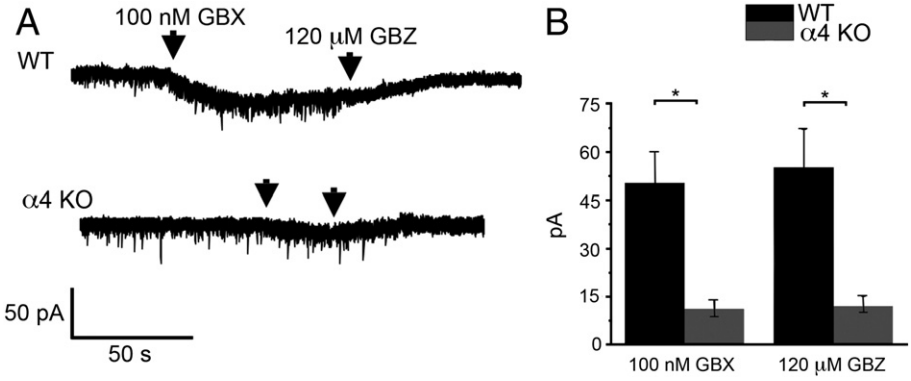

Fig. 5 – Reduced gaboxadol responsiveness of α4 KO pubertal mouse hippocampus as compared to WT pubertal mouse. The GABAR agonist gaboxadol (GBX) is selective for δ-containing GABAR at a concentration of 100 nM, while gabazine (GBZ) is an antagonist specific to all GABARs at a concentration of 120 μM. Representative currents (panel A) and averaged population data (panel B) reveal that the response to GBX was greater at puberty in WT hippocampus than in α4 KO hippocampus. The response to 120 μM GBZ is the current deflection after treatment with GBX. (*$p < 0.05$), n = 5 cells per group. Scale bar = 50 pA, 50 s.

GABAR subunits. While it has been established that the majority of GABARs released from the endoplasmic reticulum for insertion and stabilization in the plasma membrane are fully formed pentamers, it is possible for other non-typical GABARs to traffic to the plasma membrane (Bencsits et al., 1999; Connolly et al., 1996; Kittler et al., 2002; Olsen and Sieghart, 2009).

Our EM-ICC data revealed that there were δ-containing GABARs localized to the plasma membrane in pubertal α4 KO mice, albeit at a lower level as compared to pubertal WT mice. Furthermore, our electrophysiology data show, using a selective pharmacological test (100 nM GBX), that δ-containing GABARs are present, but markedly reduced, in hippocampal slices from α4 KO mice as compared to those from WT mice. Therefore, the possible interpretation we favor is the following: in the absence of α4 subunits, the δ subunit can form a full pentamer with the α1 and β subunits and that these localize to extrasynaptic sites of the plasma membrane. However, because this pentamer is not a favored GABAR composition, levels of plasma membrane insertion of putative α1βδ GABARs at puberty are much less than those for the α4βδ GABARs in WT tissue.

3.3. *α4 knockout does not impair the rise of intracellular δ in the CA1 hippocampus at the onset of puberty*

Electron microscopic analysis revealed that knockout of the α4 subunit does not affect intracellular stores of the δ subunit. In both WT and α4 KO pubertal sections, we found equivalent levels of intracellular stores of the δ subunit, both in dendritic spines and shafts. This equivalent labeling for intracellular δ in dendritic spines and shafts in WT and α4 KO animals suggests that at puberty, synthesis of δ subunits is not dependent upon the presence of the α4 subunit, but that trafficking to the membrane is dependent upon α4 expression. There is a novel explanation for the source of intracellular δ subunits in dendritic spines and shafts. It is known that predominantly fully-formed GABARs are able to overcome ER retention (Connolly et al. 1996; Kittler et al. 2002). Since it has already been proposed that α1βδ GABARs are possibly expressed in the CA1 hippocampal apical dendrites, intracellular pools of δ may be representative of fully formed α1-containing GABARs. While protein synthesis is most often thought to occur in the somatic region, studies reveal that the cellular machinery required for mRNA translation has been found in both dendritic spines and shafts of the CA1 hippocampus (Chicurel et al. 1993; Bitran et al. 1999; Ostroff et al. 2002; McCarthy and Milner 2003; Wang and Tiedge 2004; Bourne et al. 2007). Therefore, it is also possible that intracellular δ expression in the distal processes of α4 KO mice is indicative of isolated δ subunits that are synthesized locally and sequestered within the ER.

3.4. *α4 KO yields larger dendritic spine and shaft profiles*

Our EM-ICC and electrophysiology data reveal decreased functional δ-containing GABARs on CA1 hippocampal pyramidal cells. As such, these pyramidal cells should exhibit an increase in excitability and a decrease in the current necessary for triggering a spike due to the decreased GABAergic inhibition they receive. Upon examining the morphology of CA1 pyramidal cells between the two genotypes, we found that pyramidal cells of α4 KO hippocampi have larger dendritic spines, as measured by spine area and membrane length, and dendritic shafts, as measured by shaft diameter, as compared to those from WT hippocampi. These findings indicate that the expression of the α4 subunit has an effect upon the size of dendritic spine and shaft profiles. Furthermore, this increase in profile size would be expected to decrease the input resistance of the pyramidal cells, thus increasing the current necessary for triggering the neuron to fire a spike. Therefore, it is possible that neurons are undergoing a compensatory change in profile size in response to the decreased inhibition caused by α4 KO.

3.5. *Potential functional outcomes of α4 KO*

It has been reported that certain learning deficits are observed at the onset of puberty (Johnson and Newport, 1989; McGivern et al., 2002). Previous research from our laboratory has shown that increased plasmalemmal localization of α4βδ GABARs on CA1 hippocampal pyramidal cells increases the shunting, tonic inhibition and impairs activation of NMDA receptors (Shen et al, 2010). This leads to an impairment in the induction of long-term potentiation and a decline in spatial memory at the onset of puberty (Shen et al., 2010). Furthermore, when δ KO mice were tested for their spatial learning abilities, we found that the pubertal spatial learning deficit was eliminated in these mice (Shen et al., 2010). The EM-ICC and physiology data from the present study show that, in the absence of the α4 subunit, the δ subunit shows minimal plasmalemmal localization on pyramidal cells, both on CA1 dendritic shaft and spine profiles. Therefore, based on this finding, we would expect the spatial learning decline observed at the onset of puberty in WT female mice to also be eliminated in α4 KO mice.

Additional research from this laboratory has shown that α4βδ GABARs on pyramidal cells of the CA1 hippocampus mediate an increase in stress steroid-induced anxiety-like behaviors at the onset of puberty (Shen et al., 2007). The release of the progesterone metabolite, THP, is known to occur in response to stress (Girdler and Klatzkin, 2007; Purdy et al., 1991). In adults, neurosteroids such as THP acts to subsequently reduce the anxiety-inducing effects of stress (Bitran et al., 1999) by potentiating most GABARs (Belelli et al., 2002; Bianchi and Macdonald, 2003; Brown et al., 2002; Wohlfarth et al., 2002). However, the effect of THP on α4βδ GABARs is uniquely polarity-dependent, such that it increases inward current (outward flux of Cl^-), but decreases outward current (inward flux of Cl^-) at this receptor subunit combination (Shen et al., 2007). THP has been shown to rapidly desensitize outward current gated by α4βδ GABARs expressed in human embryonic kidney cells (HEK-293) (Shen et al., 2007). At puberty, when plasmalemmal localization of α4βδ GABARs is increased on CA1 hippocampal pyramidal cells, where GABAergic current is outward, THP administration reduces the shunting tonic inhibition produced by these receptors, thereby increasing the excitability of hippocampal neurons and of anxiety-like behaviors (Shen et al., 2007, 2010). Our EM-ICC and physiology data report limited localization of the δ subunit to the plasma membrane upon elimination of α4

subunit expression. Therefore, due to the absence of α4βδ GABARs, we would expect THP to diminish stress-induced excitability of CA1 pyramidal neurons and of anxiety-like behaviors, much like what is observed in adult mice (Bitran et al., 1999). In addition to mediating stress steroid anxiety responses, α4βδ GABARs are also increased by neuronal activity and traumatic brain injury (Mtchedlishvili et al., 2010; Payne et al., 2008; Santhakumar et al., 2010), which suggests they may also serve a neuroprotective role (Santhakumar et al., 2010).

The data presented here suggest that α4 subunit expression strongly affects the increases in the plasmalemmal δ subunit localization at the onset of puberty. While the mechanisms which underlie α4βδ GABAR expression at puberty have not yet been elucidated, recent work by other labs has described some of the molecular mechanisms of α4 promoter regulation, which can involve brain derived neurotrophic factor (BDNF) and heat shock proteins (Pignataro et al., 2007; Roberts et al., 2006). These findings may have relevance for alterations in mood and learning reported across fluctuations in ovarian hormones not only at pubertal onset, but also across the estrous and menstrual cycles, during and after pregnancy, and at menopause.

4. Experimental procedures

4.1. *Experimental subjects*

Twenty pubertal (36 to 43 days old) female mice were housed on a 12-h reverse light–dark cycle. α4 KO mice were generated as described previously (Chandra et al., 2006). Heterozygous α4 KO mice on a C57BL/6J × Strain 129X1/S1 genetic background of the F6 generation were imported from the University of Pittsburgh. Heterozygous mice were bred and offspring were genotyped using Southern blot analysis, as described previously (Chandra et al., 2006). Homozygous offspring were subsequently bred with each other to produce the α4 KO mice used for EM-ICC and slice electrophysiology in this study. C57BL/6J WT mice used for EM-ICC and slice electrophysiology were purchased from Jackson Laboratories (Bar Harbor, Maine). For EM-ICC analysis, mice from single shipments from Jackson Laboratories were perfused for pubertal time-points.

Female mice were chosen for use in this study because our previous findings showing increased α4βδ GABAR expression were noted in females. Vaginal opening was used to determine the onset of puberty because this physical sign is directly correlated with the hormonal changes that trigger α4βδ GABAR expression (Shen et al., 2007). Pubertal mice were used after the emergence of the vaginal opening. At these ages, the stage of the estrous cycle does not affect expression of the α4 and δ subunits (Shen et al., 2010). Five WT pubertal, and five α4 KO pubertal mice were utilized in this study for EM-ICC. An additional 5 α4 KO pubertal and 5 WT pubertal mice were used for slice electrophysiology.

All procedures involving live animals were in accordance with NIH guidelines and the Institutional Animal Care and Use Committees of SUNY Downstate Medical Center, University of Pittsburgh, and New York University Washington Square Campus.

4.2. *Characterization of antibodies*

The α4 antibody utilized in our experiments was purchased from Santa Cruz Biotechnology (catalog #sc-7355). This antibody was an affinity-purified goat polyclonal antibody directed against the extracellular N-terminus (amino acids 32–50) of the human origin peptide sequence. The α4 antibody used has been characterized previously (Griffiths and Lovick, 2005a,b; Sanna et al., 2003). On western blots, this antibody has been shown to recognize a single protein of the appropriate molecular weight (Griffiths and Lovick 2005a; Sanna et al 2003). Ultimate proof of antibody specificity using tissue from α4 KO mice had not yet been performed, and the results of such an experiment are described in this manuscript.

The δ primary antibody utilized in our experiments was obtained as a generous gift from W. Sieghart (Medical University Vienna). This antibody was an affinity purified rabbit polyclonal antibody directed against the extracellular N-terminus (amino acids 1–44) of the rat origin peptide sequence. The δ antibody used has been characterized previously by western blot analysis, in which it recognized a single band of the appropriate molecular weight (Fritschy and Mohler, 1995; Jechlinger et al., 1998). In brains from δ KO mice, no immunoreactivity was observed using the same antibody batch as was utilized in these experiments, indicating antibody specificity for the target antigen (Peng et al., 2002).

The GluR2/3 (Millipore catalog #AB1506) and MAP2 (Boehringer Mannheim Biochemicals catalog #1284 959) primary antibodies utilized in our experiments were affinity-purified. Each antibody has been extensively characterized, and recognizes a single protein of the appropriate molecular weight.

4.3. *Preparation of brain tissue for EM analysis*

All mice were anesthetized with 20% urethane (0.05–0.2 mL intraperitoneally) from 30 min to 3 h before the onset of the dark stage of the circadian cycle and perfused transcardially using a peristaltic pump (flow rate 30 mL/min), first with saline containing heparin (1 U/mL) followed by 360 mL of 4% paraformaldehyde buffered to pH 7.4 with 0.1 M phosphate buffer (PB) over a 12-min period. The brains were removed from their skulls and stored in the same fixative until sectioning, which occurred within one week after perfusion. Urethane was chosen as an anesthetic, rather than Nembutal, because Nembutal predominantly targets GABA receptors, the subject of this study, while urethane targets multiple neurotransmitter systems in a more balanced fashion (Hara and Harris, 2002).

All procedures involving transcardial perfusion of animals were carried out in accordance with the NIH guidelines and were approved by the New York University and SUNY Downstate Animal Care and Use Committees.

4.4. *Preparation of sections for immunocytochemistry*

The tissue processing protocols described previously were followed (Aoki et al., 2000). Coronal sections were cut on a vibratome (Leica VT 100 M) at a thickness of 40 μm, then stored at 4 °C in a buffer that contained 0.01 M PB with 0.9% sodium chloride (PBS), supplemented with 0.05% sodium azide to

prevent bacterial growth. Sections containing dorsal hippocampus were selected for immunocytochemical analysis. Prior to the immunocytochemical procedure, sections were freeze–thaw permeabilized, then treated with 1% hydrogen peroxide (H_2O_2) at room temperature for 30 min to retrieve antigenicity, and blocked in 0.01 M PBS supplemented with 1% bovine serum albumin and 0.05% sodium azide (PBS/BSA/Azide) for 30 min.

4.5. *Use of light microscopy*

In order to gain an initial insight into the α4 immunoreactivity in α4 KO tissue, sections were analyzed qualitatively by light microscopy (LM) using silver-intensified gold (SIG) as the immunolabel. LM allowed for assessment of global expression level changes in α4 immunoreactivity. For LM analysis, the ability to identify individual cell types (pyramidal cells, interneurons, and glia) due to contrast generated by the presence of immunoreactivity was used as evidence of expression of the α4 subunit.

LM was also utilized to assess CA1 hippocampal neuronal morphology. Immunoreactivity for the neuronal markers GluR2/3 and MAP2 allowed for characterization of neuronal phenotype and proper stratification of the CA1 hippocampus.

4.6. *Choice of immunolabels*

Labeling for the α4 and δ subunits is readily detectable in both dendritic spine profiles and apical dendritic shafts of CA1 hippocampal pyramidal cells at the onset of puberty using SIG as an immunolabel for electron microscopy (Shen et al., 2010). Therefore, we utilized this immunolabel for our electron microscopic analysis. Because SIG is a particulate label, levels of immunoreactivity are clearly quantifiable and resolvable as plasmalemmal versus intracellular with respect to its location. Furthermore, due to the lack of diffusion of SIG particles, labeling can be characterized as occurring synaptically or extrasynaptically. However, due to the lack of enzymatic amplification of the marker, this results in a very high threshold for detection.

Horseradish peroxidase-diaminobenzidine (HRP-DAB) was chosen as an immunolabel for the neuronal markers MAP2 and GluR2/3. Due to the enzymatic amplification step of HRP-DAB labeling, immunoreactivity could be readily detected at the LM level. Furthermore, the diffuse nature of HRP-DAB provides a more complete saturation of cell labeling, allowing for better structural resolution.

4.7. *Procedure using horseradish peroxidase-diaminobenzidine (HRP-DAB) as the immunolabel for light microscopy*

Sections were incubated overnight at room temperature in a primary antibody directed against the GluR2/3 subunit of AMPA receptors (1.5 μg/ml) or MAP2 (5 μg/ml), using PBS/BSA/Azide as the diluent. Sections were then rinsed, and incubated in 2° antibody for 3 h at room temperature (biotinylated anti-rabbit IgG, 1:200 for GluR2/3 1° antibody; biotinylated anti-mouse IgG, 1:200 for MAP2 1° antibody, Vector), followed by Vector's ABC mix ('Elite' kit) for 30 min. The HRP reaction used 0.3% DAB with 0.003% H_2O_2 as a substrate, stopped at 10 min with PBS rinses. Sections were dehydrated serially with ethanol, defatted with xylene, mounted on slides, and coverslipped for light microscopic analysis. All steps in the immunocytochemical procedure were conducted in parallel for WT and α4 KO tissue.

4.8. *Procedure using silver-intensified gold (SIG) as the immunolabel for electron microscopy*

Sections were incubated overnight at room temperature in a primary antibody directed against the α4 subunit (1:100 dilution from 0.2 μg/ml) or the δ subunit (1:400 dilution from 0.23 μg/ml), using PBS/BSA/Azide as the diluent. Sections were then incubated in 0.8 nm colloidal gold-conjugated 2° antibody for a minimum of 3 h at room temperature (horse-anti-goat IgG, 1:100 for α4 immunocytochemistry; goat-anti-rabbit IgG, 1:100 for δ immunocytochemistry, EM Sciences), followed by post-fixation in 2% glutaraldehyde in PBS for 10 min. Prior to the silver intensification step, sections were rinsed for 1 min in a 0.1 M citric acid buffer (trisodium citrate salt adjusted to pH 7.4 with monohydrate citric acid salt) to remove phosphate and Cl^- ions. Silver IntensEM kit (KPL, Kirkegaard & Perry Laboratories, Inc.) was applied for 10–12 min. The silver intensification reaction was terminated by a brief citrate buffer rinse, followed by PBS rinses. Ultrastructure and SIG particles were preserved using several post-fixation steps that avoid the use of osmium tetroxide: 1% tannic acid for 40 min, 1% uranyl acetate for 40 min, and 0.5% iridium tetrabromide for 20 min, all dissolved in 0.1 M maleate buffer (maleic acid monosodium salt adjusted to pH 6.0 with maleic acid disodium salt). Vibratome sections were further processed with incubation in 1% *p*-phenylenediamine for 15 min and 1% uranyl acetate overnight, both dissolved in 70% ethanol (Phend et al., 1995). Sections were then dehydrated serially with ethanol and acetone, and infiltrated with EPON-812 (EMScience), first in a 1:1 concentration with acetone, then in full EPON-812. Sections were flat embedded between sheets of Aclar plastic, and ultrathin sectioned at a thickness of 70± 1.5 nm, as measured using the minimum folds method, and collected on formvar-coated, 200-mesh EM grids. Grids were counterstained with 2% lead citrate for 30 s to increase contrast prior to imaging. All steps in the immunocytochemical procedure were conducted in parallel and with the experimenter blind to the genotype of the tissue source.

4.9. *Selection of the CA1 hippocampal region for the electron microscopic study*

In order to obtain data from a more uniform population of dendritic spine profiles, EM analysis was restricted to the dorsal CA1 hippocampal pyramidal cell apical dendrites in stratum radiatum. Schaffer collateral input from the CA3 terminates on dendritic spine profiles of the stratum radiatum (Megas et al., 2001; Smith et al., 2003). This region was chosen due to the role that hippocampal GABAR expression plays in the alterations in mood, spatial learning, and neuronal excitability that occur at the onset of puberty (Shen et al., 2007; 2010).

4.10. *Dendritic spine analysis*

For dendritic spine analysis, spine profiles were identified by the presence of an excitatory synaptic junction. These asymmetric synapses were composed of an electron dense postsynaptic density (PSD) on one side of the synapse, which was

immediately opposed by a presynaptic terminal, containing clusters of small, round, clear synaptic vesicles. It has been demonstrated extensively that dendritic spines are biological entities capable of acting autonomously of one another regardless of arising from the same parent dendrite (Carter et al., 2007; Matsuzaki et al., 2004; Yuste and Denk, 1995). Therefore, measurements of α4 and δ immunoreactivity in spines were pooled from hippocampi from multiple mice. A spine was considered labeled for the GABAR subunit when it contained even a single SIG particle. Plasmalemmal labeling was distinguished from intracellular labeling when the SIG was in contact with the plasma membrane of the spine head. A minimum of 380 μm^2 of neuropil containing at least 110 independent spine profiles was sampled from each mouse for analysis of α4 and δ immunoreactivity within dendritic spines.

4.11. *Dendritic shaft analysis*

CA1 hippocampal apical dendrites were imaged for the dendritic shaft analysis. Apical dendrites were identified by their parallel protrusion from pyramidal cells into the stratum radiatum. Dendritic shaft membranes were considered labeled when SIG particles were found in contact with the plasma membrane, as this labeling is indicative of potentially functional receptors. Labeling was characterized as synaptic when it occurred directly opposed to the presynaptic terminal, and perisynaptic when it occurred within one axon terminal's width of the presynaptic terminal. All labeling outside of these margins was characterized as extrasynaptic. The total membrane lengths of dendritic shafts were measured using the segmented line tool of ImageJ software (NIH version 10.2), and labeling was quantified as the number of immunolabeled clusters occurring per μm of dendritic plasma membrane, also referred to as linear density. A minimum of 1597 μm^2 of hippocampal neuropil containing at least 20 dendrites was sampled for each mouse for α4 and δ dendritic shaft analysis.

4.12. *Image acquisition*

The surface-most portion of vibratome sections from each mouse was examined for labeling on a JEOL transmission electron microscope (1200 EX II), as determined by proximity to the tissue-EPON interface, to ensure adequate antibody exposure. Images were digitally acquired (AMT) under identical conditions across genotypes, using a CCD camera (Hamamatsu) at magnifications of 20,000× (for dendritic shaft analysis) and 40,000× (for dendritic spine analysis). For dendritic spine analysis, non-overlapping images from the CA1 stratum radiatum were acquired. For dendritic shaft analysis, images of at least 20 pyramidal cell apical dendrites per mouse were acquired. The experimenter remained blind to the genotype of the tissue source throughout image acquisition and analysis.

4.13. *Capturing and reproduction of figures*

Electron microscopic images were captured and stored using the CCD camera attached to the JEOL 1200XL via software developed by AMT. Light microscopic images were captured at a magnification of 20× using a CCD camera attached to a Zeiss Axiophot microscope. For reproduction, a subset of these images was adjusted in contrast, brightness, and image size using Adobe Photoshop (v. CS3).

4.14. *Hippocampal slice electrophysiology*

250 μm-thick hippocampal slices were generated on a Leica oscillating microtome as described previously (Shen et al., 2007). Pyramidal cells in the CA1 hippocampal slices were visualized using a Leica DIC-infrared upright microscope, and recorded using whole cell patch clamp procedures in both voltage and current clamp modes. Patch pipets were fabricated from borosilicate glass using a Flaming-Brown puller (Sutter Instruments) to yield open tip release of 2–4 MΩ. Bath solution contained (in mM): NaCl 124, KCl 5, $CaCl_2$ 2, KH_2PO_4 1.25, $MgSO_4$ 2, $NaHCO_3$ 26 and glucose 10, saturated with 95% O_2, 5% CO_2 and buffered to pH 7.4. Recordings were carried out at room temperature (22–24 °C) at a 10 kHz sampling frequency (2 kHz 4-pole Bessel filter) using an Axopatch 200B amplifier (Axon Instruments) and pClamp 9.2 software. Electrode capacitance and series resistance were monitored and compensated. Access resistance was monitored throughout the experiment, and cells discarded if the access resistance was greater than 10 MΩ.

The pipet solution consisted of (in mM): CsCl 140, $MgCl_2$ 2, HEPES 10, BAPTA 10, Mg-ATP 2, $CaCl_2$-H_2O 0.5, Li-GTP 0.5, pH 7.2, 290 mOsm. Voltage clamp recordings were carried out at a −60 mV holding potential. In order to determine the effect of 100 nM GBX (Sigma) and 120 μM GBZ (Sigma) on the tonic inhibitory current, drugs were bath-applied after 15–20 min of recording baseline current in the presence of 2 mM kynurenic acid (Sigma). Responses were assessed by the shift in the holding current.

4.15. *Statistics*

All statistical analyses for EM-ICC and physiological experiments were performed using the Statistica program (Statsoft). The Shapiro–Wilks W-test was used to determine if the data were normally distributed. When the data were found not to be normally distributed, the Mann–Whitney *U*-test was subsequently employed to determine significance. When data were normally distributed, Student's *t*-test was employed to determine significance. For all statistical analyses, significance was accepted for $p<0.05$.

Acknowledgments

We thank Dr. Werner Sieghart for providing the δ antibody, Tunazzina Ahmed and Gauri Wable for technical assistance, and Tara Chowdhury for reading the manuscript.

Role of the funding source

This research was supported by NEI Core grant EY13079 and Klarman Family Grants Program in Eating Disorders Research and 1R21MH091445-01 to C.A., NIH Grant AA10422 to G.H., and NIH Grants DA09618 and AA12958 to S.S.S.

Contributors

Nicole Sabaliauskas performed the EM-ICC studies, Hui Shen performed the electrophysiology study, Gregg Homanics created and provided the α4 KO mice, Sheryl Smith contributed

to the experimental design and oversaw electrophysiology experiments, and Chiye Aoki contributed the experimental design and oversaw EM-ICC experiments. All authors read and approved the final draft of the manuscript.

REFERENCES

Aoki, C., Rodrigues, S., Kurose, H., 2000. Use of electron microscopy in the detection of adrenergic receptors. Methods Mol. Biol. 126, 535–563.

Bencsits, E., Ebert, V., Tretter, V., Sieghart, W., 1999. A significant part of native $GABA_A$ receptors containing $\alpha4$ subunits do not contain γ or δ subunits. J. Biol. Chem. 274, 19613–19616.

Belelli, D., Casula, A., Ling, A., Lambert, J., 2002. The influence of subunit composition on the interaction of neurosteroids with $GABA_A$ receptors. Neuropharmacology 43, 651–661.

Bianchi, M., Macdonald, R., 2003. Neurosteroids shift partial agonist activation of $GABA_A$ receptor channels from low- or high-efficacy gating patterns. J. Neurosci. 23, 10934–10943.

Bitran, D., Dugan, M., Renda, P., Ellis, R., Foley, M., 1999. Anxiolytic effects of the neuroactive steroid pregnanolone (3α-hydroxy-5β-pregnan-20-one) after microinjection in the dorsal hippocampus and lateral septum. Brain Res. 850, 217–224.

Bourne, J., Sorra, K., Hulburt, J., Harris, K., 2007. Polyribosomes are increased in spines of CA1 dendrites 2 h after the induction of LTP in mature rat hippocampal slices. Hippocampus 17, 1–4.

Brooks-Kayal, A., Shumate, M., Jin, H., Rikhter, T., Coulter, D., 1998. Selective changes in single cell $GABA_A$ receptor subunit expression and function in temporal lobe epilepsy. Nat. Med. 4, 1166–1172.

Brown, N., Kerby, J., Bonnert, T.P., Whiting, P.J., Wafford, K.A., 2002. Pharmacological characterization of a novel cell line expressing human $\alpha4\beta3\delta$ $GABA_A$ receptors. Br. J. Pharmacol. 136, 965–974.

Carter, A.G., Soler-Llavina, G.J., Sabatini, B.L., 2007. Timing and location of synaptic inputs determine modes of subthreshold integration in striatal medium spiny neurons. J. Neurosci. 27, 8967–8977.

Chandra, D., Jia, F., Liang, J., Peng, Z., Suryanarayanan, A., Werner, D.F., Spigelman, I., Houser, C.R., Olsen, R.W., Harrison, N.L., Homanics, G.E., 2006. $GABA_A$ receptor $\alpha4$ subunits mediate extrasynaptic inhibition in thalamus and dentate gyrus and the action of gaboxadol. Proc. Natl. Acad. Sci. U. S. A. 103, 15230–15235.

Chicurel, M.E., Terrian, D.M., Potter, 1993. mRNA at the synapse: analysis of a synaptosomal preparation enriched in hippocampal dendritic spines. J. Neurosci. 13, 41054–4063.

Connolly, C.N., Krishek, B.J., McDonald, B.J., Smart, T.G., Moss, S.J., 1996. Assembly and cell surface expression of heteromeric and homomeric $GABA_A$ receptors. J. Biol. Chem. 271, 89–96.

Fritschy, J.M., Mohler, H., 1995. $GABA_A$ receptor heterogeneity in the adult rat brain: differential regional and cellular distribution of seven major subunits. J. Comp. Neurol. 359, 154–194.

Girdler, S., Klatzkin, R., 2007. Neurosteroids in the context of stress: implications for depressive disorders. Pharmacol. Ther. 116, 125–139.

Glykys, J., Mody, I., 2006. Hippocampal network hyperactivity after selective reduction of tonic inhibition in $GABA_A$ receptor $\alpha5$ subunit-deficient mice. J. Neurophysiol. 95, 2796–2807.

Glykys, J., Peng, Z., Chandra, D., Homanics, G., Houser, C., Mody, I., 2007. A new naturally occurring $GABA_A$ receptor subunit partnership with high sensitivity to ethanol. Nat. Neurosci. 10, 40–48.

Goodkin, H., Joshi, S., Mtchedlishvili, Z., Brar, J., Kapur, J., 2008. Subunit-specific trafficking of $GABA_A$ receptors during status epilepticus. J. Neurosci. 28, 2527–2538.

Green, W.N., Millar, N.S., 1995. Ion-channel assembly. Trends Neurosci. 18, 280–287.

Griffiths, J., Lovick, T., 2005a. Withdrawal from progesterone increases expression of $\alpha4$, $\beta1$, and δ $GABA_A$ receptor subunits in neurons in the periaqueductal gray matter in female Wistar rats. J. Comp. Neurol. 486, 89–97.

Griffiths, J.L., Lovick, T.A., 2005b. GABAergic neurones in the rat periaqueductal grey matter express $\alpha4$, $\beta1$ and δ $GABA_A$ receptor subunits: plasticity of expression during the estrous cycle. Neuroscience 136, 457–466.

Gulinello, M., Gong, Q.H., Li, X., Smith, S.S., 2001. Short-term exposure to a neuroactive steroid increases $\alpha4$ $GABA_A$ receptor subunit levels in association with increased anxiety in the female rat. Brain Res. 910, 55–66.

Hara, K., Harris, R.A., 2002. The anesthetic mechanism of urethane: the effects on neurotransmitter-gated ion channels. Anesth. Analg. 94, 313–318 table of contents.

Hsu, F.-C., Smith, S., 2003. Progesterone withdrawal reduces paired-pulse inhibition in rat hippocampus: dependence on $GABA_A$ receptor $\alpha4$ subunit upregulation. J. Neurophysiol. 89, 186–198.

Jechlinger, M., Pelz, R., Tretter, V., Klausberger, T., Sieghart, W., 1998. Subunit composition and quantitative importance of hetero-oligomeric receptors: $GABA_A$ receptors containing $\alpha6$ subunits. J. Neurosci. 18, 2449–2457.

Johnson, J.S., Newport, E.L., 1989. Critical period effects in second language learning: the influence of maturational state on the acquisition of English as a second language. Cogn. Psychol. 21, 60–99.

Jones, A., Korpi, E., McKernan, R., Pelz, R., Nusser, Z., Mäkelä, R., Mellor, J., Pollard, S., Bahn, S., Stephenson, F., Randall, A., Sieghart, W., Somogyi, P., Smith, A., Wisden, W., 1997. Ligand-gated ion channel subunit partnerships: $GABA_A$ receptor $\alpha6$ subunit gene inactivation inhibits δ subunit expression. J. Neurosci. 15, 1350–1362.

Kittler, J., McAinsh, K., Moss, S., 2002. Mechanisms of $GABA_A$ receptor assembly and trafficking: implications for the modulation of inhibitory neurotransmission. Mol. Neurobiol. 26, 251–268.

Laurie, D.J., Seeburg, P.H., Wisden, W., 1992. The distribution of 13 $GABA_A$ receptor subunit mRNAs in the rat brain. II. Olfactory bulb and cerebellum. J. Neurosci. 12, 1063–1076.

Liang, J., Cagetti, E., Olsen, R., Spigelman, I., 2004. Altered pharmacology of synaptic and extrasynaptic $GABA_A$ receptors on CA1 hippocampal neurons is consistent with subunit changes in a model of alcohol withdrawal and dependence. J. Pharmacol. Exp. Ther. 310, 1234–1245.

Liang, J., Suryanarayanan, A., Chandra, D., Homanics, G., Olsen, R., Spigelman, I., 2008. Functional consenquences of $GABA_A$ receptor $\alpha4$ subunit deletion on synaptic and extrasynaptic currents in the mouse dentate granule cells. Alcohol. Clin. Exp. Res. 32, 19–26.

Liang, J., Zhang, N., Cagetti, E., Houser, C., Olsen, R., Spigelman, I., 2006. Chronic intermittent ethanol-induced switch of ethanol actions from extrasynaptic to synaptic hippocampal $GABA_A$ receptors. J. Neurosci. 26, 1749–1758.

Maguire, J., Stell, B., Rafizadeh, M., Mody, I., 2005. Ovarian cycle-linked changes in $GABA_A$ receptors mediating tonic inhibition alter seizure susceptibility and anxiety. Nat. Neurosci. 8, 797–804.

Maguire, J., Ferando, I., Simonsen, C., Mody, I., 2009. Excitability changes related to $GABA_A$ receptor plasticity during pregnancy. J. Neurosci. 29, 9592–9601.

Matsuzaki, M., Honkura, N., Ellis-Davies, G.C., Kasai, H., 2004. Structural basis of long-term potentiation in single dendritic spines. Nature 429, 761–766.

McCarthy, J.B., Milner, T., 2003. Dendritic ribosomes suggest local protein synthesis during estrous synaptogenesis. NeuroReport 14, 1357–1360.

McGivern, R., Andersen, J., Byrd, D., Mutter, K., Reilly, J., 2002. Cognitive efficiency on a match to sample task decreases at the onset of puberty in children. Brain Cogn. 50, 73–89.

Meera, P., Wallner, M., Otis, T., 2011. Molecular basis for the high THIP/gaboxadol sensitivity of extrasynaptic $GABA_A$ receptors. J. Neurophysiol. July 27.

Megas, M., Emri, Z., Freund, T.F., Gulys, A.I., 2001. Total number and distribution of inhibitory and excitatory synapses on hippocampal CA1 pyramidal cells. Neuroscience 102, 527–540.

Mtchedlishvili, Z., Lepsveridze, E., Xu, H., Kharlamov, E., Lu, B., Kelly, K., 2010. Increase of $GABA_A$ receptor-mediated tonic inhibition in dentate granule cells after traumatic brain injury. Neurobiol. Dis. 38, 464–475.

Nusser, Z., Sieghart, W., Stephenson, F.A., Somogyi, P., 1996. The α6 subunit of the $GABA_A$ receptor is concentrated in both inhibitory and excitatory synapses on cerebellar granule cells. J. Neurosci. 16, 103–114.

Nusser, Z., Sieghart, W., Somogyi, P., 1998. Segregation of different $GABA_A$ receptors to synaptic and extrasynaptic membranes of cerebellar granule cells. J. Neurosci. 18, 1693–1703.

Olsen, R., Sieghart, W., 2009. $GABA_A$ receptors: subtypes provide diversity of function and pharmacology. Neuropharmacology 56, 141–148.

Ostroff, L., Fiala, J., Allwardt, B., Harris, K., 2002. Polyribosomes redistribute from dendritic shafts into spines with enlarged synapses during LTP in developing rat hippocampal slices. Neuron 35, 535–545.

Payne, H., Ives, J., Sieghart, W., Thompson, C., 2008. AMPA and kainate receptors mediate mutually exclusive effects on $GABA_A$ receptor expression in cultured mouse cerebellar granule neurones. J. Neurochem. 104, 173–186.

Peng, Z., Hauer, B., Mihalek, R., Homanics, G., Sieghart, W., Olsen, R., Houser, C., 2002. $GABA_A$ receptor changes in delta subunit-deficient mice: altered expression of α4 and γ2 subunits in the forebrain. J. Comp. Neurol. 446, 179–197.

Phend, K.D., Rustioni, A., Weinberg, R.J., 1995. An osmium-free method of epon embedment that preserves both ultrastructure and antigenicity for post-embedding immunocytochemistry. J. Histochem. Cytochem. 43, 283–292.

Pignataro, L., Miller, A., Ma, L., Midha, S., Protiva, P., Herrera, D., Harrison, N., 2007. Alcohol regulates gene expression in neurons via activation of heat shock factor 1. J. Neurosci. 27, 12957–12966.

Pirker, S., Schwarzer, C., Wieselthaler, A., Sieghart, W., Sperk, G., 2000. $GABA_A$ receptors: immunocytochemical distribution of 13 subunits in the adult rat brain. Neuroscience 101, 815–850.

Purdy, R.H., Morrow, A.L., Moore, P.H., Paul, S.M., 1991. Stress-induced elevations of $GABA_A$ receptor-active steroids in the rat brain. Proc. Natl. Acad. Sci. U. S. A. 88, 4553–4557.

Roberts, D., Hu, Y., Lund, I., Brooks-Kayal, A., Russerk, S., 2006. Brain-derived neurotrophic factor (BDNF)-induced synthesis of early growth response factor (Egr3) controls the level of type A GABA receptor α4 subunits in hippocampal neurons. J. Biol. Chem. 281, 29431–29435.

Sanna, E., Mostallino, M., Busonero, F., Talani, G., Tranquilli, S., Mameli, M., Spiga, S., Follesa, P., Biggio, G., 2003. Changes in $GABA_A$ receptor gene expression associated with selective alterations in receptor function and pharmacology after ethanol withdrawal. J. Neurosci. 23, 11711–11724.

Santhakumar, V., Jones, R., Mody, I., 2010. Developmental regulation and neuroprotective effects of striatal tonic $GABA_A$ currents. Neuroscience 167, 644–655.

Shen, H., Gong, Q., Yuan, M., Smith, S., 2005. Short-term steroid treatment increases δ $GABA_A$ receptor subunit expression in rat CA1 hippocampus: pharmacological and behavioral effects. Neuropharmacology 49, 573–586.

Shen, H., Gong, Q., Aoki, C., Yuan, M., Ruderman, Y., Dattilo, M., Williams, K., Smith, S., 2007. Reversal of neurosteroid effects at $\alpha4\beta2\delta$ $GABA_A$ receptors triggers anxiety at puberty. Nat. Neurosci. 10, 469–477.

Shen, H., Sabaliauskas, N., Sherpa, A., Fenton, A., Stelzer, A., Aoki, C., Smith, S., 2010. A critical role for $\alpha4\beta\delta$ $GABA_A$ receptors in shaping learning deficits at puberty in mice. Science 327, 1515–1518.

Smith, M., Ellis-Davies, G.C.R., Magee, J., 2003. Mechanism of the distance-dependent scaling of Schaffer collateral synapses in rat CA1 pyramidal neurons. J. Physiol. 548, 245–258.

Smith, S.S., Gong, Q.H., Hsu, F.C., Markowitz, R.S., ffrench Mullen, J.M., Li, X., 1998b. $GABA_A$ receptor α4 subunit suppression prevents withdrawal properties of an endogenous steroid. Nature 392, 926–930.

Smith, S.S., Gong, Q.H., Li, X., Moran, M., Bitran, D., Frye, C., Hsu, F.-C., 1998a. Withdrawal from 3α-OH-5α-pregnan-20-one using a pseudopregnancy model alters the kinetics of hippocampal $GABA_A$-gated current and increases the $GABA_A$ receptor α4 subunit in association with increased anxiety. J. Neurosci. 18, 5275–5284.

Sperk, G., Schwarzer, C., Tsunashima, K., Fuchs, K., Sieghart, W., 1997. $GABA_A$ receptor subunits in the rat hippocampus I: immunocytochemical distribution of 13 subunits. Neuroscience 80, 987–1000.

Staley, K., Mody, I., 1992. Shunting of excitatory input to dentate gyrus granule cells by a depolarizing $GABA_A$ receptor-mediated postsynaptic conductance. J. Neurophysiol. 68, 197–212.

Stell, B., Mody, I., 2002. Receptors with different affinities mediate phasic and tonic $GABA_A$ conductances in hippocampal neurons. J. Neurosci. 22, RC223.

Studler, B., Fritschy, J.M., Brnig, I., 2002. GABAergic and glutamatergic terminals differentially influence the organization of GABAergic synapses in rat cerebellar granule cells *in vitro*. Neuroscience 114, 123–133.

Sundstrom-Poromaa, I., Smith, D., Gong, Q., Sabado, T., Li, X., Light, A., Wiedmann, M., Williams, K., Smith, S., 2002. Hormonally regulated $\alpha4\beta2\delta$ $GABA_A$ receptors are a target for alcohol. Nat. Neurosci. 5, 721–722.

Sur, C., Farrar, S.J., Kerby, J., Whiting, P.J., Atack, J.R., McKernan, R.M., 1999. Preferential coassembly of α4 and δ subunits of the $GABA_A$ receptor in rat thalamus. Mol. Pharmacol. 56, 110–115.

Suryanarayanan, A., Liang, J., Meyer, E., Lindermeyer, A., Chandra, D., Homanics, G., Sieghart, Olsen, R., Spigelman, I., 2011. Subunit compensation and plasticity of synaptic $GABA_A$ receptors induced by ethanol in α4 subunit knockout mice. Front. Neurosci. Volume 5 Article 110.

Wang, H., Tiedge, H., 2004. Translational control at the synapse. The Neuroscientist 10, 456–466.

Wei, W., Faria, L., Mody, I., 2004. Low ethanol concentrations selectively augment the tonic inhibition mediated by δ subunit-containing GABAA receptors in hippocampal neurons. J. Neurosci. 24, 8379–8382.

Wei, W., Zhang, N., Peng, Z., Houser, C., Mody, I., 2003. Perisynaptic localization of δ subunit-containing $GABA_A$ receptors and their activation by GABA spillover in the mouse dentate gyrus. J. Neurosci. 23, 10650–10661.

Wisden, W., Laurie, D., Monyer, H., Seeburg, P., 1992. The distribution of 13 $GABA_A$ receptor subunit mRNAs in the rat brain. I. telencephalon, diencephalon, mesenchephalon. J. Neurosci. 12, 1040–1062.

Wohlfarth, K., Bianchi, M., Macdonald, R., 2002. Enhanced neurosteroid potentiation of ternary $GABA_A$ receptors containing the δ subunit. J. Neurosci. 22, 1541–1549.

Yuste, R., Denk, W., 1995. Dendritic spines as basic functional units of neuronal integration. Nature 375, 682–684.

Zhou, X., Smith, S., 2007. Steroid requirements for regulation of the α4 subunit of the $GABA_A$ receptor in an *in vitro* model. Neurosci. Lett. 411, 61–66.